JOTCS A
Journal of the Turkish Chemical Society
Section: A
Chemistry
TURKISH CHEMICAL SOCIETY

Recycling of Waste Polymethyl-Methacrylate as an Optical Transparent Host

Erkan Aksoy[1*]

[1]Project and Technology Office, Rectorate, Bartin University, 74100, Bartin, Türkiye.

Abstract: Reusing waste or otherwise discarded polymethyl methacrylate (wPMMA) as a host matrix for optical photonic applications such as down-conversion or luminescence solar concentrators can spare the use of pristine materials, with strong implications for sustainability. Here, a homogeneous emissive film was produced using wPMMA by dissolving in toluene and adding a fluorescent perylene dye (perylene-3,4,9,10-tetracarboxylic hexyl ester, PTHE) followed by spin coating casting. This resulting film is optically transparent and green-emissive with a high photoluminescence quantum yield (PLQY of 84%). It has been investigated by various spectroscopic techniques such as absorption, photoluminescence, emission lifetime, and dye photostability. While this film exhibited some excimer PL at longer wavelengths compared to the solution phase, it also increased its emission lifetime by approximately 3 times. Moreover, while the CIE coordinates (x, y) of the blue-green PL in the solution phase was 0.21, 0.56, the PL spectrum of the wPMMA:PTHE film instead had (CIE, x, y) of 0.30, 0.60. Recycling these and similar suitable waste polymers and transforming them into value-added products such as down-conversion or luminescent solar concentrator films can contribute to sustainable development goals within the scope of clean energy, energy efficiency, and waste utilization.

Keywords: Waste polymethyl methacrylate, optical host, recovery of waste polymer, solid-state lighting, luminescence solar concentrator, perylene dye.

Submitted: December 30, 2023. **Accepted:** June 21, 2024.

Cite this: Aksoy E. Recycling of Waste Polymethyl-Methacrylate as an Optical Transparent Host. JOTCSA. 2024;11(3): 1141-50.

DOI: https://doi.org/10.18596/jotcsa.1412323

***Corresponding author's E-mail:** eaksoy@bartin.edu.tr

1. INTRODUCTION

Plastics are a wide category of synthetic materials composed of chains or networks (polymers) of repeating smaller building blocks (monomers). Plastics typically possess exceptional versatility, allowing them to be shaped into various forms without compromising on durability, flexibility, lightweight nature, or affordability. They also enable composite production with adjustable structural and physical properties depending on different synthetic substitutions or blending with other materials (1-4). This remarkable adaptability has supported plastics finding applications in a wide range of industries since the mid-20th century, spanning from automotive and packaging to electronics and medical device manufacturing (5-8). While plastic production and usage have grown exponentially in recent decades - estimated to reach approximately 400 million tons per year – the product lifecycle of these materials is not fully developed. Approximately 12% of plastic production is disposed of by incineration, and only approximately 9% is recycled despite their chemical suitability for reuse (9). Hence, while plastics serve numerous useful purposes in modern society, most of the plastics produced remain discarded in nature for hundreds of years following use (a result of their chemical stability). This pollution contaminating environments and water resources is now an urgent environmental problem that must be addressed (10-12). Hence, efforts to recycle rather than discard plastics not only contribute to the protection of environmental and human health but also contribute to a sustainable future in terms of protecting natural resources, saving energy, combating climate change, and managing economic outputs and waste (4,13,14).

Polymethyl methacrylate (PMMA), also known as acrylic glass, is a thermoplastic polymer obtained by polymerization of methyl methacrylate (MMA) monomer (5). PMMA is used in many different areas, such as furniture, building facades, lighting

fixtures, automobiles, contact lenses, chemical tanks, and optics and photonic technologies (15). In photonic technologies specifically, PMMA is used extensively in roles such as light transport in optical fibres, eyeglasses, and telescope lenses, LCD (liquid crystal display) and LED (light emitting diode) screen protectors, dye hosts for light conversion layers in blue LEDs, and optical filter production (5,7,16-24). All these features and application areas make PMMA an important plastic group in this technological field. However, PMMA has low biodegradability in waste environments, and its production processes have several environmental impacts to consider - such as the necessity of using water in its production, the production of MMA from oil and natural gas, and energy consumption – which establish the importance of PMMA recycling and (re)use.

Perylene derivatives are known for their strong light absorption in the visible region and high fluorescence quantum yields. In addition, since they exhibit high optical, electrochemical, and thermal stability, perylene dyes are used in many optical or optoelectronic technologies such as (organic) light emitting diodes (LEDs and OLEDs), organic solar cells (OSCs), luminescent solar concentrators (LSC), lasers, ion sensing, and phototherapy (25-34). Perylene tetra esters contain the same planar polycyclic aromatic core but typically suffer significant aggregation caused by quenching (ACQ) of their emission in the film phase (35,36). Two basic approaches to eliminate or alleviate ACQ are to synthesize perylene derivatives with steric functional groups that reduce the aggregation effect (35,37,38), or by doping and isolating low concentrations of perylene derivatives into optically transparent host materials, in both cases increasing the intermolecular distance (34,37). This second approach, in particular, allows these ACQ-prone dyes to be used in high-efficiency applications such as wavelength-converting lighting technologies and solar concentrators (34,39).

In this study, we show that waste/discarded PMMA polymer (wPMMA) can be reclaimed as an optically transparent host for Perylene-3,4,9,10-tetracarboxylic hexyl ester (PTHE), doped at 1 wt% and with optoelectronic applications as outlined above. Due to the environmental and economic impacts of waste polymers, this technique can contribute to the Sustainable Development Goals (40) and reduce the need for additional PMMA production from petrochemicals. PTHE and the dye-loaded films were characterized by FTIR, ^{1}H-NMR, ^{13}C-NMR, HRMS, TGA, XRD, and optical spectroscopy. PTHE exhibited extremely high PL intensity and PLQY when homogeneously dispersed in the organic-compatible wPMMA, with excellent stability towards photoexcitation. The PTHE:wPMMA film (or others like it) can hence be used as an environmentally friendly material feedstock in the production of white light-emitting (O)LEDs or other photonics applications.

2. EXPERIMENTAL SECTION

2.1. Materials and Instruments

Perylene tetracarboxylic dianhydride (PTCDA), 1-hexanol, 1-bromohexane, 1,8-diazabicyclo[5.4.0] undec-7-ene (DBU), N,N-dimethylformamide, chloroform, toluene, silica gel and thin layer chromatography (TLC) were obtained from Sigma and Merck. The waste polymethyl methacrylate (wPMMA) used in this study (Figure 1, picture on the right) was obtained as waste from a laser-cutting stationery shop. PTHE was synthesized (Figure 2) according to the literature (21,41). The synthetic details are provided below, together with its structural, thermal, and optical characterizations.

FTIR-ATR, ^{1}H, and ^{13}C NMR spectra were obtained using IRaffinity-1 SHIMADZU-FTIR and Bruker (400 MHz and 100 MHz) spectrometers, respectively. TGA analysis was carried out with a Hitachi STA 7300 Model device with an increase of 10 °C per minute in a nitrogen atmosphere. Absorption and photoluminescence (PL), absolute PL quantum yield (ΦPL) (with an integrated sphere), time-correlated single photon count (τ, ns) (EPL-470 nm excitation) studies and photostability testing were performed with the Analytical Jena S600 UV–Vis spectrophotometer and Edinburgh FLS920P and FS5 Instruments.

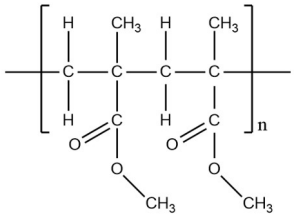

Polymethyl methacrylate
(PMAA)

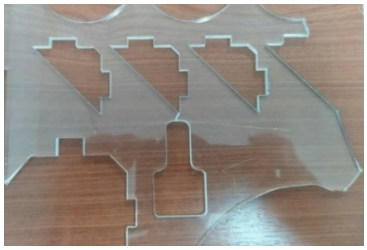

Figure 1: Molecular structure of polymethyl methacrylate (left) and available waste polymethyl methacrylate (wPMMA) (right).

2.2. Synthesis and Characterization of Perylene-3,4,9,10-tetracarboxylic hexyl ester (PTHE)

Perylene tetra esters emit with very high fluorescence efficiency in the solution phase (PLQY≥90%) (42). Therefore, in this study, PTHE was chosen as a reference fluorophore. Detailed information on the synthesis methods and

characterization of PTHE (Figure 1) and wPMMA:PTHE film (Figure 2) are given below (Figure 1-10).

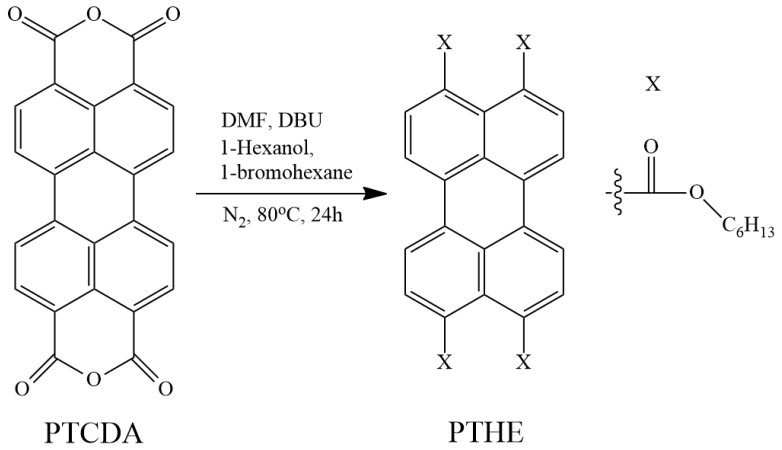

Figure 2: Reaction scheme of PTHE.

Perylene-3,4,9,10-tetracarboxylic dianhydride (PTCDA) (1 g, 2.55 mmol), N,N-dimethylformamide (DMF), 1-bromohexane (4.2 g, 25.5 mmol) and 1-hexanol (2.6 g, 25.5 mmol) were added into a two-necked round-bottomed flask. After it was stirred for 20 minutes in a magnetic stirrer, the DBU (1.5 mL) catalyst was added and stirred at 80 °C under reflux in N_2 for 24 hours. After the flask was brought to room temperature, it was poured into distilled water, and the precipitate was filtered through vacuum filter paper and washed with methanol. After drying the solid at 60 °C, it was dissolved in chloroform and purified by column chromatography over silica gel. Yield (79%) 1.54 g. FTIR (ATR) (Figure 3): υmax = (C_{Ar}-H): 2951, 2928 cm_{-1}, (C-H): 2864, 2848 cm^{-1}, (C=O): 1726, 1710 cm^{-1}, (C-O): 1263 and 746 cm^{-1}. ^{1}H-NMR (400 MHz, Chloroform-d, TMS/ppm) δ (Figure 4): 8.25-8.23 (d, J: 8.0 Hz, 4H), 8.01 7.99 (d, J: 8.0 Hz, 4H), 4.30 (t, J: 8.0 Hz, 8H), 1.77 (m, J: 8.0 Hz, 8H), 1.43 (m, J: 8.0 Hz, 8H), 1.34 (m-overlap, J:4.0 Hz, 16H), 0.89 ppm. (m, J:8.0 Hz, 12H). ^{13}C-NMR (100 MHz, Chloroform-d, TMS/ppm) δ (Figure 5): 168.48, 133.01, 130.42, 130.38, 121.35, 65.62, 31.49, 28.53, 25.65, 22.54, 14.01 ppm. HRMS (Figure 6): (Molecular mass;764.4) Found: 764.4 M. The first temperature at which PTHE begins to degrade is 349 °C (TGA) (Figure 7).

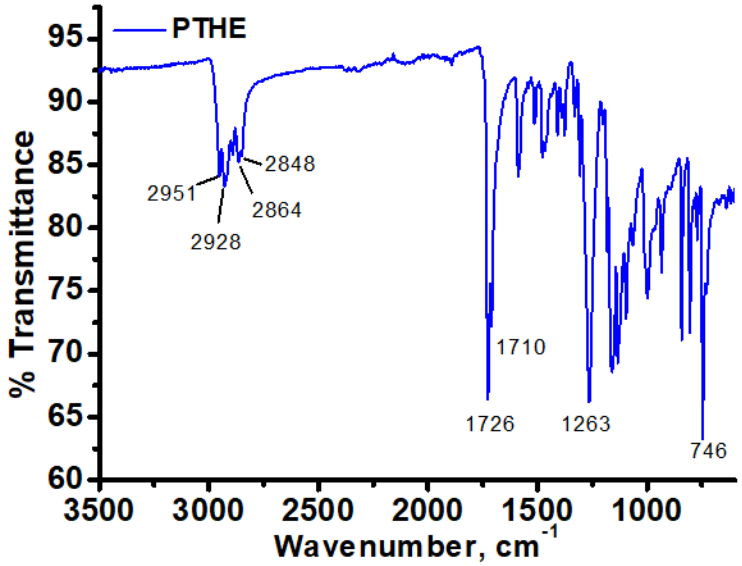

Figure 3: FTIR spectrum of PTHE.

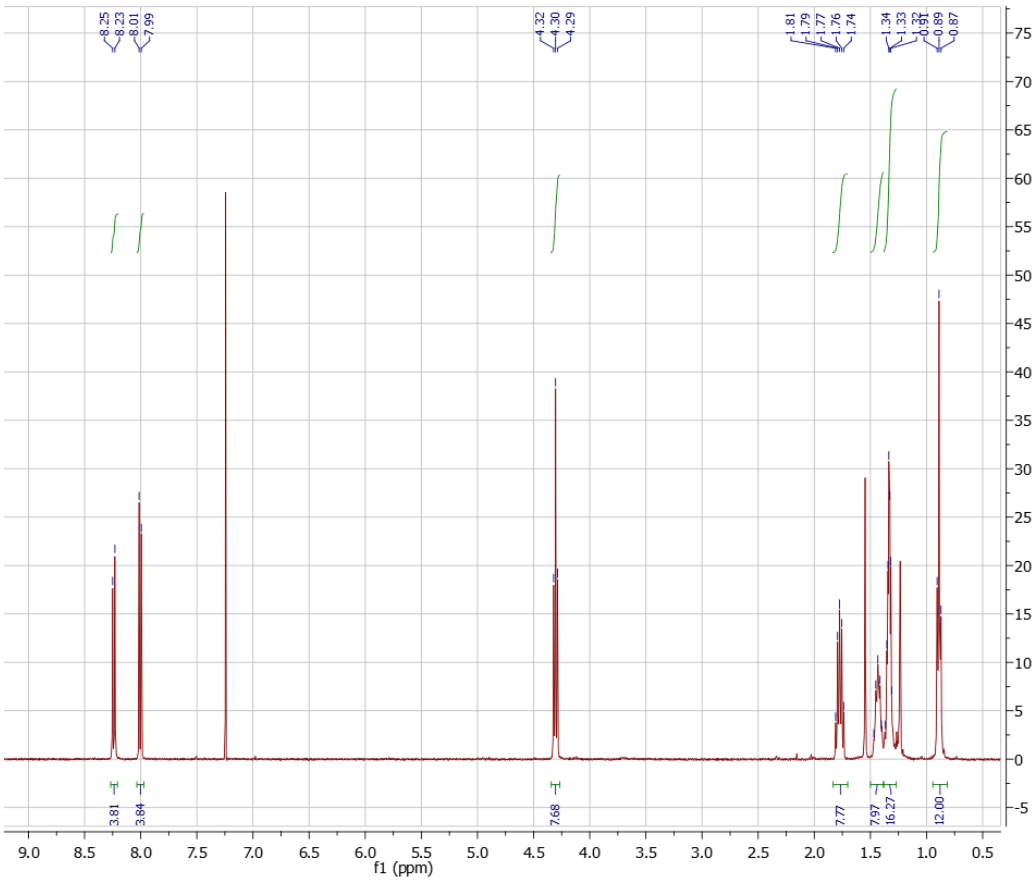

Figure 4: ^{1}H-NMR of PTHE.

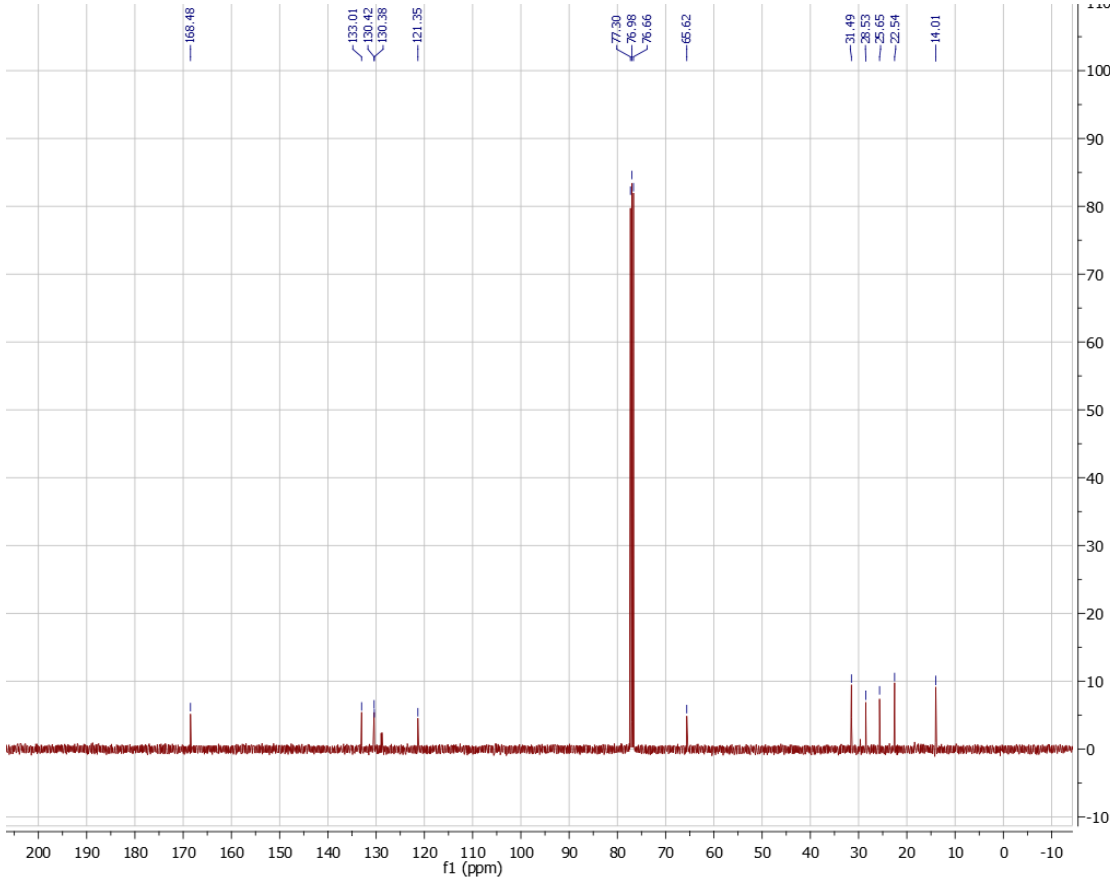

Figure 5: ^{13}C-NMR of PTHE.

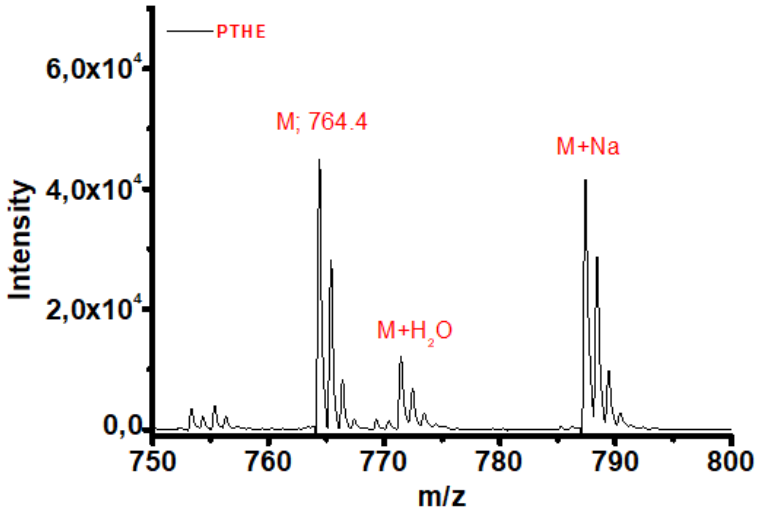

Figure 6: HRMS of PTHE.

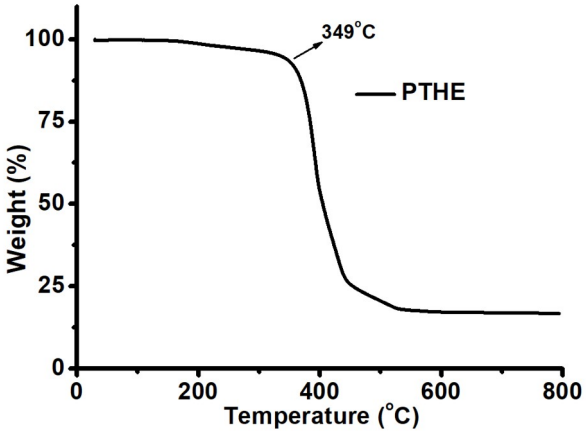

Figure 7: TGA analysis of PTHE.

2.3. Preparation and Characterization of wPMMA-PTHE Solution and Film

150 mg of wPMMA was added to a capped bottle, then 10 mL of toluene was added and stirred at 50 °C for 24 hours with a magnetic stirrer. A clear solution of wPMMA was obtained, and 1% by mass of PTHE was added to it. A homogeneous solution of wPMMA:PTHE was obtained by stirring for a further 2 hours.

100 mL of the wPMMA:PTHE toluene solution was dropped on a clean 2.5 x 2.5 cm glass tile, rotating at 2000 rpm. After this film dried, the process was repeated 10 times to build thickness, and the film was left to dry at room temperature. Pictures of the prepared transparent and green-emissive wPMMA: PTHE film under daylight and UV light are given in Figure 8.

The Fourier transform infrared (FTIR-ATR) characterization study of wPMMA:PTHE film, in comparison with PTHE and wPMMA, is given in Figure 9. Aromatic C-H peaks of PTHE are seen at 2951 cm^{-1} and 2928 cm^{-1}. C=O, which belongs to ester bonds, exhibited strong peaks at 1726 cm^{-1} and 1710 cm^{-1}. Additionally, a strong peak of C-O is observed at 1263 cm^{-1} and is compatible with the literature (42). The aliphatic C-H peak of wPMMA shows itself weakly at 2949 cm^{-1}. C=O and C-O peaks belonging to the ester structure are seen as sharp and intense at 1724 cm^{-1} and 1143 cm^{-1}, respectively. In the wPMMA:PTHE film, it has the characteristic peaks of the two materials. Due to the high PMMA ratio, wPMMA characteristic peaks are dominant. However, the presence of two new intense peaks observed at 796 cm^{-1} and 1016 cm^{-1} indicates that there is an interaction between the wPMMA and PTHE (Figure 9).

The X-ray diffractions (XRD) of PTHE powder, wPMMA, and wPMMA:PTHE are given in Figure 10. PTHE powder showed peaks at 2θ = 8,6, 10.76, 13.0, 15.36, 16.72, 17.56, 18.16, 18.44, 21.48 (intense), 23.8, 24.88, 25.56, 42.56 and 43.48. The values of the broad 2theta peaks of wPMMA and wPMMA:PTHE films are approximately 13.68 (intense), 25.0, and 42.56, respectively. It exhibited broadness, which is characteristic of wPMMA and belongs to the amorphous structure. In the wPMMA:PTHE film, 2theta peaks belonging to PTHE were not observed due to the low PTHE doping rate (Figure 10) (43).

Figure 8: Images of PTHE film (in wPMMA) under daylight and UV light.

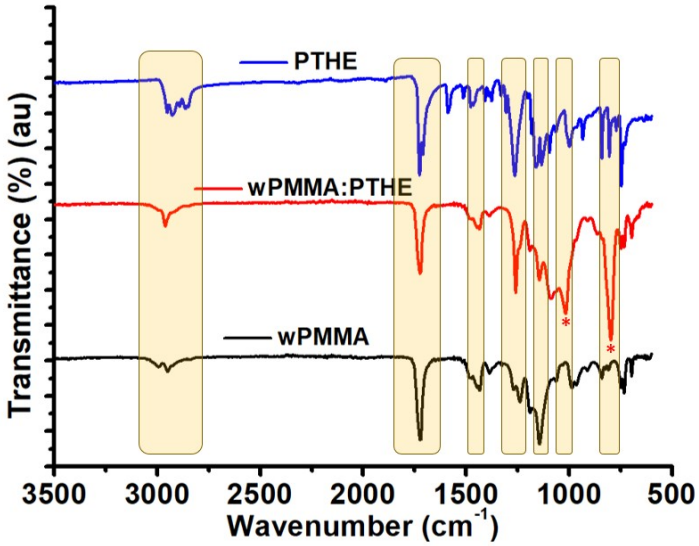

Figure 9: FTIR spectrum of PTHE powder, wPMMA and wPMMA:PTHE (99:1, wt%) films.

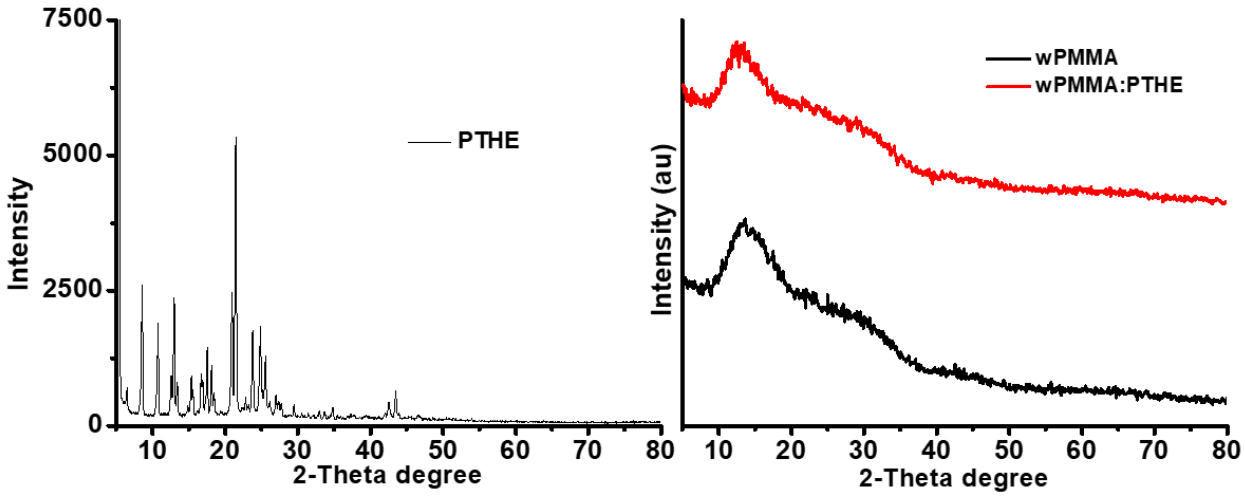

Figure 10: XRD spectrum of PTHE powder (left) and XRD spectra (au) of film phase of wPMMA and wPMMA:PTHE (99:1, wt%) (right).

3. RESULTS AND DISCUSSION

The absorption and photoluminescence spectra of PTHE in toluene [1x10^{-6} M] and in wPMMA (1 wt%) are given in Figure 11a. Dilute PTHE in toluene exhibits absorbance peaks at 474 and 445 nm belonging to the π-π* transitions associated with its extended aromatic pi system (38,42). Compared to a previously reported study (41), the absorption of PTHE is almost the same as in chloroform solution (λ_{absmax}: 472 nm). For the preparation of solid films, 1 wt% doping of PTHE into wPMMA was chosen to control aggregation of the PTHE. In the wPMMA:PTHE film the absorption peaks (λ_{absmax}) of PTHE were found to be nearly identical to the toluene solution, at 472 and 443 nm.

In the PL spectrum of PTHE, it was found that the λ_{PLmax} shifted from 492 to 525 nm on changing from solution to film measurements. PTHE is proposed to exhibited excimer behavior in wPMMA that gives rise to this wavelength shift, motivated by fact that there was no significant difference in the absorption spectrum (that might indicate ground-state aggregate formation) and that the PL spectrum exhibited only a single peak at longer wavelengths. Emission lifetime measurements of the solution and wPMMA:PTHE film were also performed, it was

determined that the average lifetime of the PL at 525 nm in the film was extended from 3.8 to 12.1 ns (Figure 11b and Table 1). When examined in more detail, while PTHE had a single exponential state in solution, it exhibited a double exponential state in the film phase (at 525 nm). The first exponential state is similar to the situation in solution, with an exciton lifetime of 3.77 ns and a relative contribution of 61.71% to the total emission (Table 1). The second decay component instead has a lifetime of 15.38 ns, and a relative contribution of 38.38%. This second emission component with increased lifetime indicates the existence of excimeric states, with no impact on the absorption spectrum. When reported neat-film emission spectra of similar PTE derivatives of different chain lengths are examined, the presence of PL from aggregates leads to shifting to much longer wavelengths (≈ 600 nm) (44).

The longer wavelength excimer emission in the film phase also increases the Stokes shift compared to the monomeric behaviour in dilute solution (shifts of 772 and 2139 cm^{-1}), significantly reducing reabsorption of PTHE in the film phase. Indeed, the absolute PLQY (Φ) in the film is quite high, as in solution: 98 and 84% in solution and film, respectively (Table 1). Commission Internationale de l'eclairage (CIE) chromaticity coordinates of the PL spectra are shown in Figure 11c, with the excimer emission providing a slightly different emission colour point for the film. The PL_{max} intensity of the film, which was exposed to the excitation wavelength at its maximum absorption in the kinetic mode of the Edinburgh FS5 fluorometer for 90 minutes, was measured at 525 nm every second and exhibited a highly photostable behavior (Figure 11d).

Table 1: Average lifetime value (τ) of wPTHE in toluene ($1x10^{-6}$ M) and at film phase (%1 doped in wPTHE).

PTHE	τ_1 (ns)	%	τ_2 (ns)	%
In toluene	3.80	100	-	-
In wPMMA	3.77	61.71	15.38	38.29

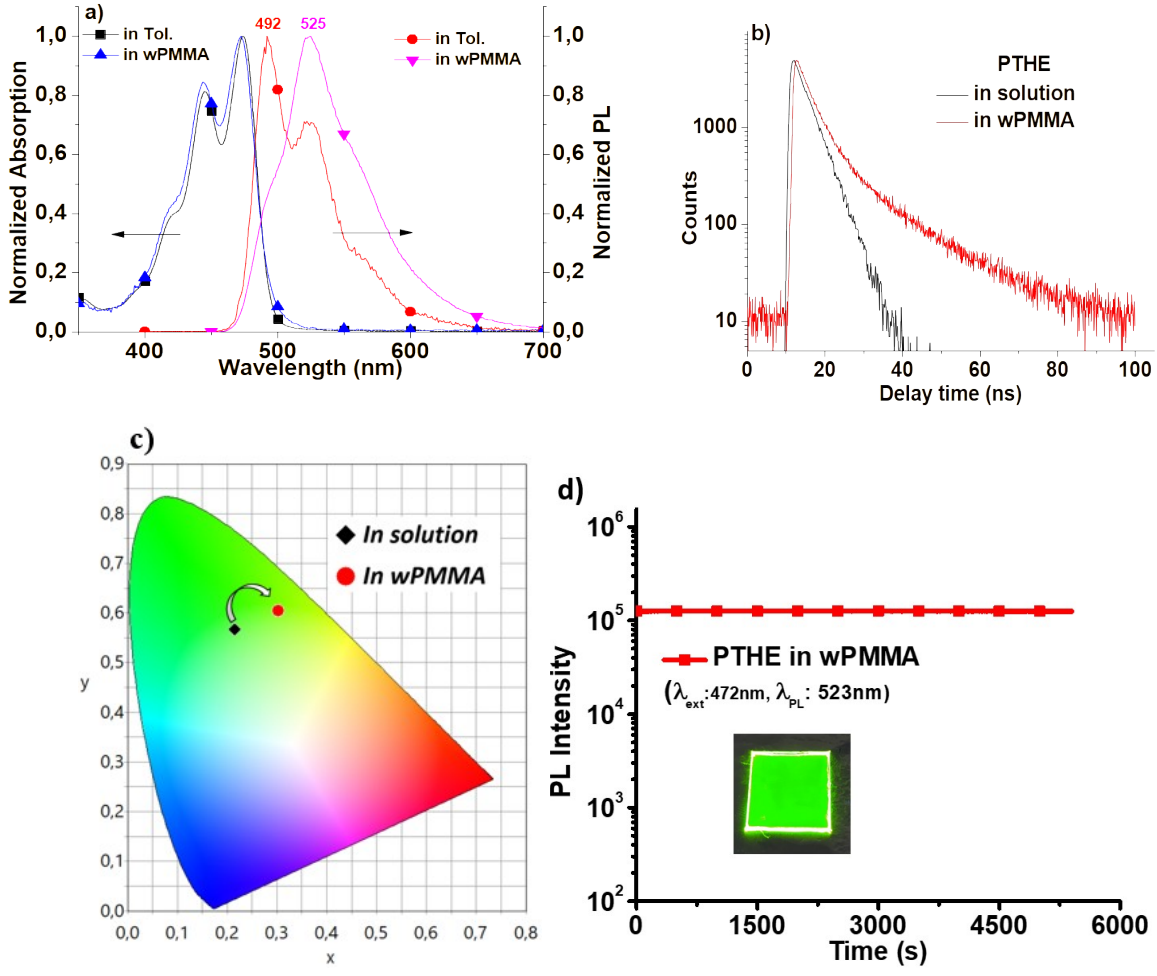

Figure 11: a) Absorption and PL spectra of PTHE in solution and film phase. b) Lifetime decay of PTHE in solution and wPMMA (%1 doped PTHE). c) CIE diagrams of PL spectra of PTHE in toluene ($1x10^{-6}$ M) and in wPMMA. d) Optical stability test of PTHE.

Table 2: Photophysical properties of PTHE in toluene [1x10^{-6} M] and film (in wPMMA) [maximum absorption, λ_{abs}^{max} and maximum PL, λ_{PL}^{max} peaks (nm); Stokes shift, $\Delta\lambda$ (nm and cm^{-1}); PLQY, (Φ%).

	In toluene [1x10^{-6}]				In wPMMA (1%)			
	λ_{abs}^{max}	λ_{PL}^{max}	$\Delta\lambda$ (nm) or (cm^{-1})	Φ %	λ_{abs}^{max}	λ_{PL}^{max}	$\Delta\lambda$ (nm) or (cm^{-1})	Φ%
PTHE	474	492	18 nm or 772 cm^{-1}	98	472	525	53 nm or 2139 cm^{-1}	84

4. CONCLUSION

The increasing use of plastics and the resulting serious environmental threat they pose must be addressed by all means available. In this study, solutions of waste PMMA were combined with an organic dye to produce green-emissive films suitable for photonics applications. Reprocessing such waste into high-value products may contribute to SDG goals and services within the scope of a sustainable future, clean energy, and energy efficiency (40).

PTHE, which is homogeneously dispersed in waste PMMA, absorbs blue light in the range of 400-500 nm when only 1% is added while also exhibiting a very high fluorescence quantum yield. Reusing waste PMMA with different combinations of fluorophores in this way could open the door to its use in many photonic technologies that absorb, transform, or emit wavelengths.

5. ACKNOWLEDGMENTS

The author would like to thank Dr. Andrew Danos for his support of this work and suggestions.

6. REFERENCES

1. Fan LT, Retzloff DG, Vanderpool WO. Solid waste-plastics composites. Physical properties and feasibility for production. Environ Sci Technol [Internet]. 1972 Dec 1;6(13):1085–91. Available from: <URL>.

2. Bossa N, Sipe JM, Berger W, Scott K, Kennedy A, Thomas T, et al. Quantifying mechanical abrasion of mwcnt nanocomposites used in 3d printing: Influence of cnt content on abrasion products and rate of microplastic production. Environ Sci Technol [Internet]. 2021 Aug 3;55(15):10332–42. Available from: <URL>.

3. Jiang H, Zhang Y, Wang H. Surface reactions in selective modification: The prerequisite for plastic flotation. Environ Sci Technol [Internet]. 2020 Aug 18;54(16):9742–56. Available from: <URL>.

4. Shamsuyeva M, Endres HJ. Plastics in the context of the circular economy and sustainable plastics recycling: Comprehensive review on research development, standardization and market. Compos Part C Open Access [Internet]. 2021 Oct;6:100168. Available from: <URL>.

5. Ali U, Karim KJBA, Buang NA. A Review of the properties and applications of poly (methyl methacrylate) (PMMA). Polym Rev [Internet]. 2015 Oct 2;55(4):678–705. Available from: <URL>.

6. Yaqoob L, Noor T, Iqbal N. Conversion of plastic waste to carbon-based compounds and application in energy storage devices. ACS Omega [Internet]. 2022 Apr 26;7(16):13403–35. Available from: <URL>.

7. Santidrián A, Sanahuja O, Villacampa B, Diez JL, Benito AM, Maser WK, et al. Chemical postdeposition treatments to improve the adhesion of carbon nanotube films on plastic substrates. ACS Omega [Internet]. 2019 Feb 28;4(2):2804–11. Available from: <URL>.

8. Wang Y, Wang H, Li S, Sun S. Waste PET Plastic-derived CoNi-based metal–organic framework as an anode for lithium-ion batteries. ACS Omega [Internet]. 2022 Oct 4;7(39):35180–90. Available from: <URL>.

9. Tsakona M, Baker E, Rucevska I, Maes T, Appelquist R, Macmillan-Lawler M, et al. Drowning In plastics – marine litter and plastic waste vital graphics [Internet]. United Nations Environment Programme. 2021. 6–77 p. Available from: <URL>.

10. Jambeck JR, Geyer R, Wilcox C, Siegler TR, Perryman M, Andrady A, et al. Plastic waste inputs from land into the ocean. Science (80-) [Internet]. 2015 Feb 13;347(6223):768–71. Available from: <URL>.

11. Barnes DKA, Galgani F, Thompson RC, Barlaz M. Accumulation and fragmentation of plastic debris in global environments. Philos Trans R Soc B Biol Sci [Internet]. 2009 Jul 27;364(1526):1985–98. Available from: <URL>.

12. Authors R, Brighty:, Jones GC, V4 RJ. High-level science review for "A Plastic Oceans" film contents section [Internet]. 2016. Available from: <URL>.

13. Al-Salem SM, Lettieri P, Baeyens J. Recycling and recovery routes of plastic solid waste (PSW): A review. Waste Manag [Internet]. 2009 Oct;29(10):2625–43. Available from: <URL>.

14. Naderi Kalali E, Lotfian S, Entezar Shabestari M, Khayatzadeh S, Zhao C, Yazdani Nezhad H. A critical review of the current progress of plastic waste recycling technology in structural materials. Curr Opin Green Sustain Chem [Internet]. 2023 Apr;40:100763. Available from: <URL>.

15. Manoukian OS, Sardashti N, Stedman T, Gailiunas K, Ojha A, Penalosa A, et al. Biomaterials for tissue engineering and regenerative medicine. In: Encyclopedia of Biomedical Engineering [Internet]. Elsevier; 2019. p. 462–82. Available from: <URL>.

16. Deka N, Bera A, Roy D, De P. Methyl methacrylate-based copolymers: Recent developments in the areas of transparent and stretchable active matrices. ACS Omega [Internet]. 2022 Oct 25;7(42):36929–44. Available from: <URL>.

17. Li Y, Wang YQ, Liu D, Gao Y, Wang SN, Qiu H. Dual-emission ratiometric fluorescent probe based on lanthanide-functionalized carbon quantum dots for white light emission and chemical sensing. ACS Omega [Internet]. 2021 Jun 8;6(22):14629–38. Available from: <URL>.

18. El-Bashir SM. Enhanced fluorescence polarization of fluorescent polycarbonate/zirconia nanocomposites for second generation luminescent solar concentrators. Renew Energy [Internet]. 2018 Jan;115:269–75. Available from: <URL>.

19. El-Bashir SM. Coumarin-doped PC/CdSSe/ZnS nanocomposite films: A reduced self-absorption effect for luminescent solar concentrators. J Lumin [Internet]. 2019 Feb;206:426–31. Available from: <URL>.

20. Al-Mahdouri A, Gonome H, Okajima J, Maruyama S. Theoretical and experimental study of solar thermal performance of different greenhouse cladding materials. Sol Energy [Internet]. 2014 Sep;107:314–27. Available from: <URL>.

21. Aksoy E, Demir N, Varlikli C. White LED light production using dibromoperylene derivatives in down conversion of energy. Can J Phys [Internet]. 2018 Jul;96(7):734–9. Available from: <URL>.

22. Coffey B, Clough L, Bartkus DD, McClellan IC, Greenberg MW, LaFratta CN, et al. Photophysical properties of cyclometalated platinum(II) diphosphine compounds in the solid state and in pmma films. ACS Omega [Internet]. 2021 Oct 26;6(42):28316–25. Available from: <URL>.

23. Langhals H, Schlücker T, Reiners F, Karaghiosoff K. Terminal terthiophenediones: fast-decay fluorescent dyes and their efficient syntheses. ACS Omega [Internet]. 2021 Sep 28;6(38):24973–80. Available from: <URL>.

24. Sengottuvelu D, Shaik AK, Mishra S, Ahmad H, Abbaszadeh M, Hammer NI, et al. Multicolor nitrogen-doped carbon quantum dots for environment-dependent emission tuning. ACS Omega [Internet]. 2022 Aug 9;7(31):27742–54. Available from: <URL>.

25. Fang H, Xia D, Zhao C, Zhou S, Wang R, Zang Y, et al. Perylene bisimides-based molecular dyads with different alkyl linkers for single-component organic solar cells. Dye Pigment [Internet]. 2022 Jul;203:110355. Available from: <URL>.

26. Zheng X, Wei Q, Shan T, Zhang Y, Zhong H. The halogen effect of perylene diimide-based non-fullerene acceptors on photovoltaic properties. Dye Pigment [Internet]. 2022 May;201:110232. Available from: <URL>.

27. Keum C, Becker D, Archer E, Bock H, Kitzerow H, Gather MC, et al. Organic light-emitting diodes based on a columnar liquid-crystalline perylene emitter. Adv Opt Mater [Internet]. 2020 Sep 15;8(17):2000414. Available from: <URL>.

28. Ostos FJ, Iasilli G, Carlotti M, Pucci A. High-Performance luminescent solar concentrators based on poly(cyclohexylmethacrylate) (PCHMA) films. Polymers (Basel) [Internet]. 2020 Dec 3;12(12):2898. Available from: <URL>.

29. Schiphorst J ter, Kendhale AM, Debije MG, Menelaou C, Herz LM, Schenning APHJ. Dichroic perylene bisimide triad displaying energy transfer in switchable luminescent solar concentrators. Chem Mater [Internet]. 2014 Jul 8;26(13):3876–8. Available from: <URL>.

30. Szukalska A, Szukalski A, Stachera J, Zajac D, Chrzumnicka E, Martynski T, et al. Perylene-based chromophore as a versatile dye for light amplification. Materials (Basel) [Internet]. 2022 Jan 27;15(3):980. Available from: <URL>.

31. Liu Y, Wang K, Guo D, Jiang B. Supramolecular assembly of perylene bisimide with β-cyclodextrin grafts as a solid-state fluorescence sensor for vapor detection. Adv Funct Mater [Internet]. 2009 Jul 24;19(14):2230–5. Available from: <URL>.

32. Yang N, Song S, Ren J, Liu C, Li Z, Qi H, et al. Controlled aggregation of a perylene-derived probe for near-infrared fluorescence imaging and phototherapy. ACS Appl Bio Mater [Internet]. 2021 Jun 21;4(6):5008–15. Available from: <URL>.

33. Guner T, Aksoy E, Demir MM, Varlikli C. Perylene-embedded electrospun PS fibers for white light generation. Dye Pigment [Internet]. 2019 Jan;160:501–8. Available from: <URL>.

34. Aksoy E, Danos A, Varlikli C, Monkman AP. Navigating CIE space for efficient TADF downconversion WOLEDs. Dye Pigment [Internet]. 2020 Dec;183:108707. Available from: <URL>.

35. Zhang B, Lyskov I, Wilson LJ, Sabatini RP, Manian A, Soleimaninejad H, et al. FRET-enhanced photoluminescence of perylene diimides by combining molecular aggregation and insulation. J Mater Chem C [Internet]. 2020;8(26):8953–61. Available from: <URL>.

36. Kozma E, Mróz W, Villafiorita-Monteleone F, Galeotti F, Andicsová-Eckstein A, Catellani M, et al. Perylene diimide derivatives as red and deep red-emitters for fully solution processable OLEDs. RSC Adv [Internet]. 2016;6(66):61175–9. Available from: <URL>.

37. Aksoy E, Danos A, Li C, Monkman A, Varlıklı C. The Effect of imide substituents on the excited state properties of perylene diimide derivatives. Turkish J Sci Technol [Internet]. 2022 Mar 20;17(1):11–21. Available from: <URL>.

38. Aksoy E, Danos A, Li C, Monkman AP, Varlikli C. Silylethynyl substitution for preventing aggregate

formation in perylene diimides. J Phys Chem C [Internet]. 2021 Jun 17;125(23):13041–9. Available from: <URL>.

39. Davis NJLK, MacQueen RW, Roberts DA, Danos A, Dehn S, Perrier S, et al. Energy transfer in pendant perylene diimide copolymers. J Mater Chem C [Internet]. 2016;4(35):8270–5. Available from: <URL>.

40. de Sousa FDB. The role of plastic concerning the sustainable development goals: The literature point of view. Clean Responsible Consum [Internet]. 2021 Dec;3:100020. Available from: <URL>.

41. Benning S, Kitzerow HS, Bock H, Achard MF. Fluorescent columnar liquid crystalline 3,4,9,10-tetra-(n-alkoxycarbonyl)-perylenes. Liq Cryst [Internet]. 2000 Jul;27(7):901–6. Available from: <URL>.

42. Aksoy E, Bozkus V, Varlikli C. Tuning the colour of solution processed perylene tetraester based OLEDs from yellowish-green to greenish-white: A molecular engineering approach. Dye Pigment [Internet]. 2023 Mar;211:111050. Available from: <URL>.

43. Hashem M, Rez MF, Fouad H, Elsarnagawy T, Elsharawy M, Umar A, et al. Influence of titanium oxide nanoparticles on the physical and thermomechanical behavior of poly methyl methacrylate (PMMA): A Denture Base Resin. Sci Adv Mater [Internet]. 2017 Jun 1;9(6):938–44. Available from: <URL>.

44. Piosik E, Synak A, Paluszkiewicz J, Martyński T. Concentration dependent evolution of aggregates formed by chlorinated and non-chlorinated perylene tetracarboxylic acid esters in pure spin-coated films and in a PMMA matrix. J Lumin [Internet]. 2019 Feb;206:132–45. Available from: <URL>.